Cell. Mol. Life Sci. (2015) 72:1795–1809
DOI 10.1007/s00018-014-1766-1

Cellular and Molecular Life Sciences

RESEARCH ARTICLE

Pax6 controls centriole maturation in cortical progenitors through *Odf2*

Marco A. Tylkowski · Kefei Yang · Sigrid Hoyer-Fender · Anastassia Stoykova

Received: 12 June 2014 / Revised: 14 October 2014 / Accepted: 17 October 2014 / Published online: 29 October 2014

Abstract Cortical glutamatergic neurons are generated by radial glial cells (RGCs), specified by the expression of transcription factor (TF) Pax6, in the germinative zones of the dorsal telencephalon. Here, we demonstrate that Pax6 regulates the structural assembly of the interphase centrosomes. In the cortex of the Pax6-deficient *Small eye* (*Sey*/*Sey*) mutant, we find a defect of the appendages of the mother centrioles, indicating incomplete centrosome maturation. Consequently, RGCs fail to generate primary cilia, and instead of staying in the germinative zone for renewal, RGCs detach from the ventricular surface thus affecting the interkinetic nuclear migration and they exit prematurely from mitosis. Mechanistically, we show that TF Pax6 directly regulates the activity of the *Odf2* gene encoding for the appendage-specific protein Odf2 with a role for the assembly of mother centriole. Our findings demonstrate a molecular mechanism that explains important characteristics of the centrosome disassembly and malfunctioning in developing cortex lacking Pax6.

M. A. Tylkowski · A. Stoykova (✉)
Research Group of Molecular Developmental Neurobiology, Department Molecular Cell Biology, Max-Planck Institute for Biophysical Chemistry, Am Faßberg 11, 37077 Göttingen, Germany
e-mail: astoyko@gwdg.de

M. A. Tylkowski · A. Stoykova
Center for Nanoscale Microscopy and Molecular Physiology of the Brain (CNMPB), 37075 Göttingen, Germany

K. Yang · S. Hoyer-Fender
Johann-Friedrich-Blumenbach-Institute of Zoology and Anthropology, Developmental Biology, GZMB, Ernst-Caspari-Haus, Georg-August-Universität Göttingen, Justus-von-Liebig-Weg 11, Göttingen, Germany

Keywords Centriole structure · Transcriptional control

Introduction

The complex structure of the mammalian neocortex consists of billions of neurons and glial cells generated during development by stem and progenitor cells located in the germinative zones of the dorsal telencephalon (pallium), the ventricular zone (VZ) and the subventricular zone (SVZ) [1, 2]. Before the beginning of neurogenesis, neuroepithelial cells with stem cell-like properties in VZ of cortical primordium divide in a symmetric proliferative manner to increase the progenitor pool. At the onset of neurogenesis, the neuroepithelial cells start to express some glial determinants as well as TF Pax6, and transform into radial glial cells (RGC), which produce almost all cortical glutamatergic neurons [3–8]. During neurogenesis, which in the mouse extends from embryonic stage (E)10.5 till E18.5, distinct neuronal types are produced following an intrinsic "inside-first outside-last" program [9]. At early stages (E10.5–E13.5), RGCs divide in an asymmetric differentiation manner, generating RGCs for self-renewal and neurons via a direct mode of neurogenesis. Guided by the long processes of RGCs extended across the cortical depth, the newborn neurons delaminate from the VZ and migrate into the cortical plate (CP) where they are predominantly positioned into layer six, and consequently, into layer 5 [10, 11]. However, after midgestation (E13.5), the RGCs divide asymmetrically to self-renew, producing a second type of progenitor cells, the intermediate progenitors, located in the SVZ. Here, they may undergo up to 3 divisions before entering into symmetric terminal neurogenic divisions (indirect mode of neurogenesis), generating neuronal subtypes with upper layers identities, firstly neurons of layer 4, and subsequently, layer 3 and layer 2 neurons [12–14].

The evolutionary conserved paired-domain, homeodomain containing TF *Pax6* is an important component of an encoded genetic program in cortical RGCs regulating neurogenesis, cortical arealization and layer formation [15–19]. In *Pax6* deficiency, as seen in *Pax6/Small eye* homozygous (*Sey/Sey*) mutant mice [20], the RGC produces only half of the normal number of cortical neurons [21]. Furthermore, the size of their motor and somatosensory cortex is severely diminished and the upper layer neuronal subtypes are almost completely missing [15, 18, 19, 22–28].

TF Pax6 is an intrinsic determinant of RGCs, endowing them with neurogenic ability [21, 29]. Multiple evidence indicates that *Pax6* exerts control on RGC morphology and cell cycle including cell cycle length and exit, mitotic spindle orientation, centrosome localization during mitosis and regulates the interkinetic nuclear migration [23, 24, 29–32]. The interkinetic nuclear migration is cell cycle dependent movement during which the nuclei of the apical RGCs translocate from a basal (S-phase) to an apical (M-phase) position [33]. This process is related to cell microtubules in which the centrosome, as the microtubule-organizing centre, plays a critical role [34]. The centrosome also plays important roles in the regulation of progenitor proliferation, fate determination, neuronal differentiation and migration [35]. Consisting of two centrioles, which differ in structure and function, the centrosome replicates in a cell cycle dependent semi-conservative mode [36]. As a result, only one of the centrosomes, the mother centrosome, inherits the original more mature (mother) centriole (MC). The mother centriole specifically carries distal/subdistal appendages marked by specific proteins such as Odf2 (Outer dense fibre 2/Cenexin), which is considered a molecular marker of centriole maturation, and Ninein [37–41]. After RGC division, the cell containing the mother centrosome stays in the VZ, while the cell containing the daughter centrosome (without appendages) migrates into the cortical plate upon neuronal differentiation [42]. The mother centriole is transformed into a basal body and grows a primary cilium [43, 44], which is involved in mediating signal transduction critical for normal corticogenesis [45, 46].

Here, we present evidence that TF Pax6 controls centrosome assembly in interphase RGCs. We found that Pax6 controls the transcription of the *Odf2* gene and consequently, the production of the appendage-specific protein Odf2, thereby contributing to the centriole maturation.

Results

Mislocation and loss of centrosome subdistal appendages in *Sey/Sey* cortex

During interphase, the centrosomes in RGCs are generally located at the cell membrane in the most apical region of the VZ surface. It is only during mitosis that centrosomes leave this position to build the spindle poles. To study centrosome location in *Pax6*-deficient mouse cortex, we performed immunohistochemistry (IHC) analysis of γ-Tubulin, a common centriole marker on brain cross-sections from wild-type (WT) and homozygous *Pax6/Small eye* (*Sey/Sey*) mutant embryos at stage E15.5. While in WT cortex the centrosomes were strictly aligned, seemingly anchored to the ventricular surface (Fig. 1a), in the *Pax6* deficient brain they were widely distributed within the space between the ventricular surface and the cell nuclei (Fig. 1b), which is in accordance with reported results for the rat *Small eye* mutant ($rSey^2/rSey^2$) [31]. Given the importance of the MC appendages for the connection to the cell membrane during the generation of primary cilia, we hypothesized that a structural defect of the appendages in *Pax6* loss of function (LOF) may underlay centrosome mislocation in VZ (Fig. 1c). To test this hypothesis, we investigated by electron microscopy (EM) the centrosome/basal body structure at the cortical ventricular surface in E15.5 WT (Fig. 1d–d‴) and *Sey/Sey* (Fig. 1e-e‴) embryos. As normally half of the centrioles are MC, in the control brain 51.26 % (±6.21) of the centrioles showed subdistal appendages (Fig. 1f). Strikingly less centrioles showed subdistal appendages in the *Sey/Sey* brains (21.8 % with appendages; 78.2 % without appendages; ±7.13) (Fig. 1g). Thus compared to WT, less than 50 % of the centrioles in *Pax6* deficient cortex contained appendages, suggesting a defect in centrosome maturation (Fig. 1h).

Reduction of primary cilia in *Sey/Sey* cortex

Absence of subdistal appendages has been shown to cause loss of primary cilia in mouse F9 cells [47]. To investigate whether the loss of appendages and the resulting dislocation of centrioles have an influence on the appearance of primary cilia, we analysed EM images from E15.5 cross-sections of WT and *Sey/Sey* brain sections. We found that the number of centrioles connected to primary cilia was dramatically reduced in E15.5 *Pax6* loss of function brains (Fig. 2c–d′) compared to WT (Fig. 2a–b′) (WT: 34.89 % ± 9.24; *Sey/Sey*: 6.01 ± 4.42) (Fig. 2e, f), indicating more than 80 % reduction in the mutant brain (Fig. 2g). Furthermore, IHC performed using an antibody to adenylyl cyclase III (ACIII) as a specific primary cilia marker [48] revealed a 50 % reduction in the number of primary cilia at the ventricular surface (Fig. 2h, i). Taken together, these results suggest that Pax6 disruption alters the centriole maturation in RGCs.

Abnormal localization of the mother centrosome in Pax6 deficient cortex

After mitosis, the mother centrosome locates to the RGC that re-enters the cell cycle and stays in VZ [42]. To

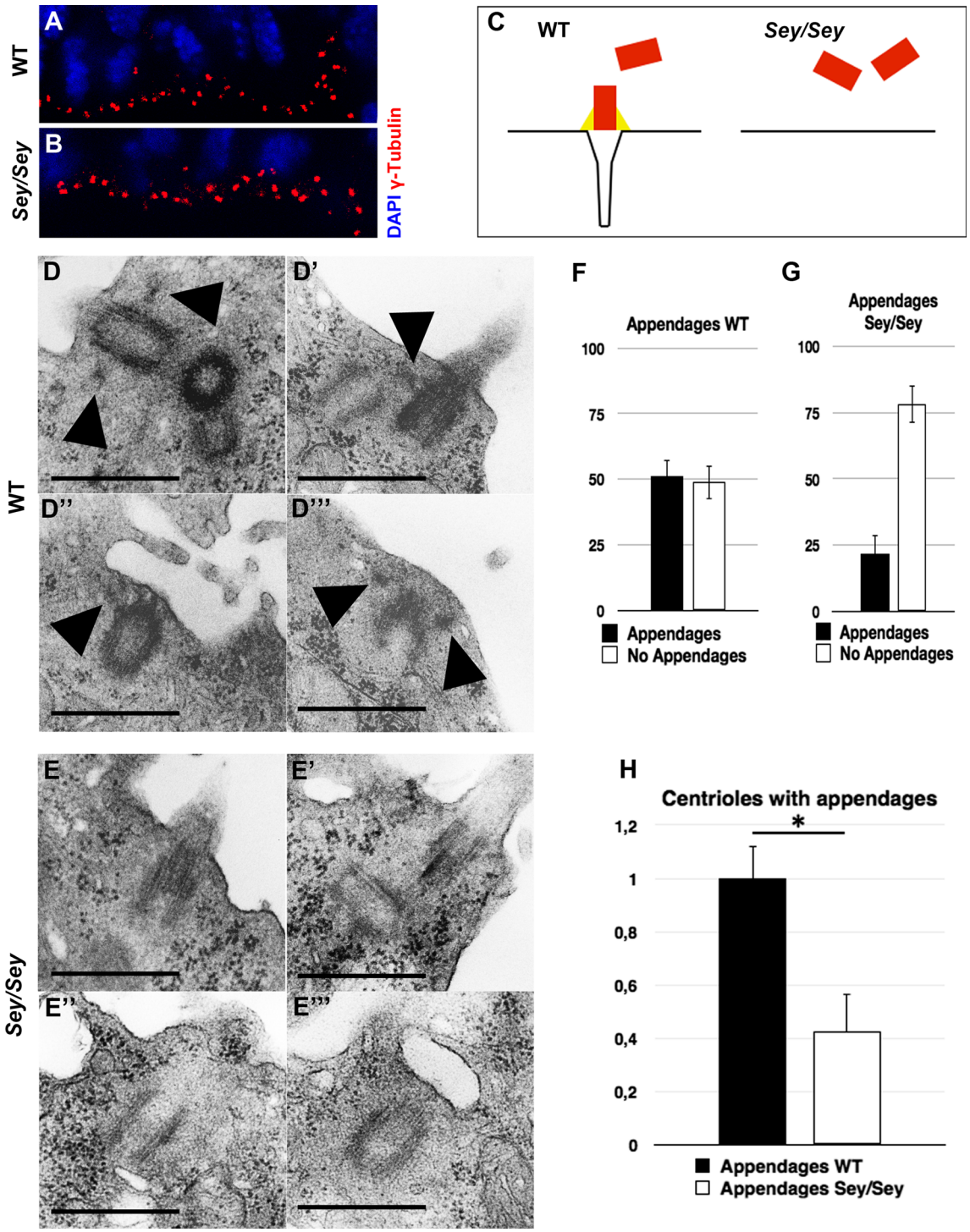

Fig. 1 Defect of centrosome maturation in Pax6-deficient cortex. **a**, **b** IHC with the centrosome marker γ-Tubulin (in *red*) in WT (**a**) and *Pax6/Small eye* (*Sey/Sey*) (**b**) E15.5 cortex reveals a disturbed localization of centrosomes in the mutant cortex. Cell nuclei are counterstained with DAPI (*blue*). **c** Schematic presentation to explain how a structural defect of the mother centriole appendages could lead to mis-localization of the centrosomes. **d**–**e**$'''$ Electron microscopy micrographs illustrating the structural defect of the mother centrioles in *Sey/Sey* (**e**–**e**$'''$) compared with WT (**d**–**d**$'''$) control cortex. *Arrowheads* point to subdistal appendages easily detectable only in WT cortex. **f**–**g** Statistical analysis of the centriole number at the ventricular surface of WT embryo showing that half of the centrioles (51.26 ± 6.21 %) contains appendages, thus identifying them as mother centrioles, and 48.74 % (±6.21) as daughter centrioles (without appendages). Note that in the *Sey/Sey* cortex only 21.8 % (±7.13) of centrioles contain appendages and 78.2 % (±7.13) miss these appendages ($n = 3$) (*bars* 0.5 μm). **h** Relative to the control, the Pax6 deficient cortex shows a strong reduction in the number of matured centrioles containing appendages at the ventricular surface (WT: 1 ± 0.12); *Sey/Sey*: 0.43 ± 0.14); *≤0.05; $p = 0.012$)

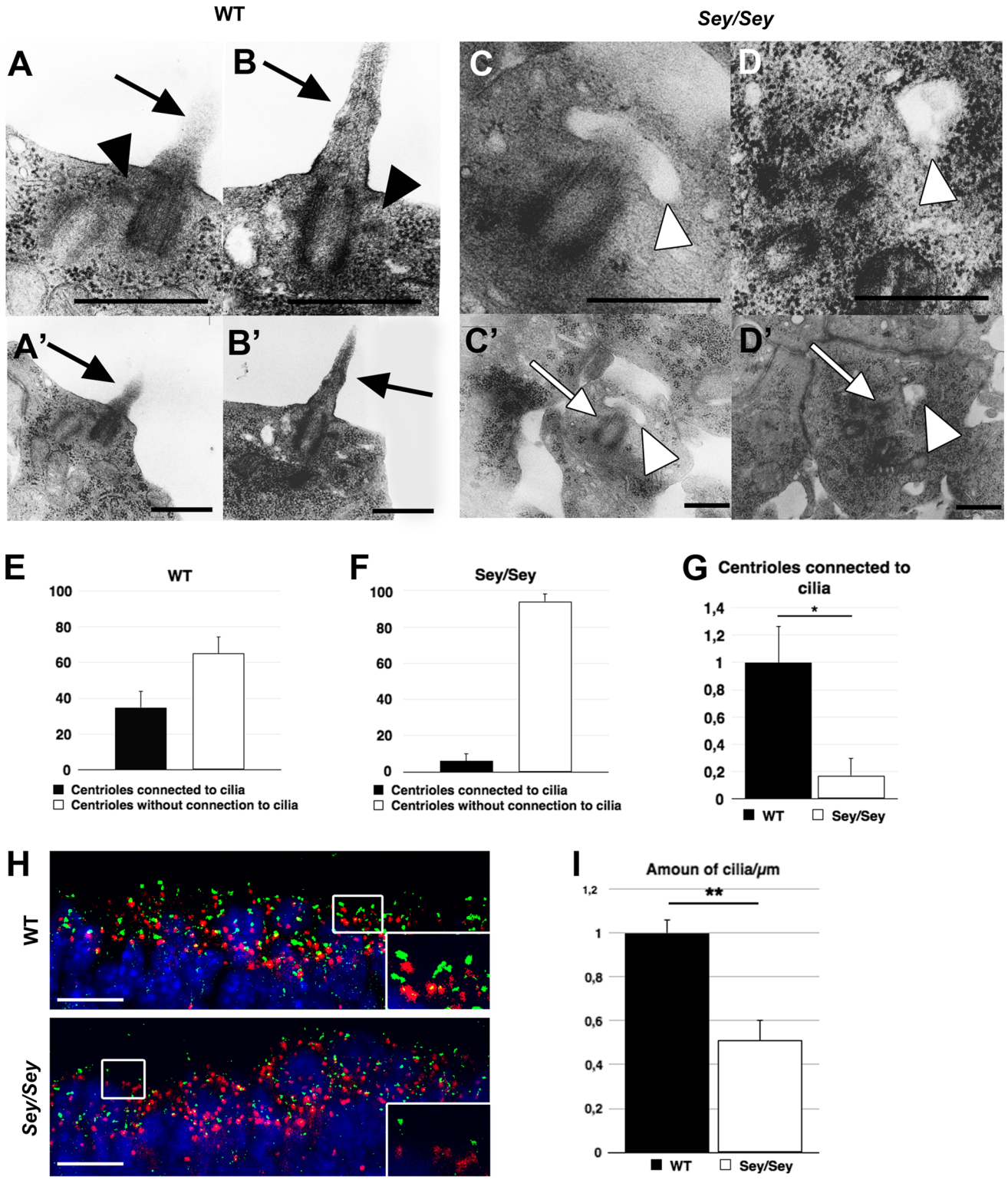

study the position of the mother centrosome in Pax6 deficiency, we applied a modified version of the published method of Imai et al. [49]; using a fluorescent photo switchable Kaede-centrin1 protein that is specifically expressed in the centrioles upon in utero electroporation into the embryonic brain. Due to severe cranial and brain defects of the *Sey/Sey* embryos, their survival upon in utero electroporation was low. We used therefore embryos after conditional deletion of Pax6 in cortical progenitors (*Pax6cKO*). *Pax6*$^{fl/fl}$ transgenic mice [50] were crossed to

◀**Fig. 2** Loss of Pax6 causes a profound reduction of centrioles connected to primary cilia at the ventricular surface. **a**, **b** WT E15.5 cortex contains centrioles, showing the characteristic appendages (*black arrowheads*), connected to primary cilia (*black arrows*) (**a**, **b**) at the ventricular surface (**a′**, **b′**). **c**, **d** Centrioles in Pax6 mutant E15.5 cortex show fewer connections to primary cilia. Instead they show characteristic vesicles at the distal end of the mother centriole (*white arrowheads*), necessary to build up the primary cilium. **c′**, **d′** The overview shows that the centrioles (*white arrows*) are located away from the ventricular surface (*bars* 0.5 µm). **e**, **f** Statistical analysis of the number of centrioles connected to primary cilia. In WT cortex around 35 % of centrioles are connected to primary cilia (34.89 ± 9.24 %), while in *Sey*/*Sey* cortex only around 6 % show this connection (6.01 ± 4.42 %). **g** Normalized to control, the number of centrioles connected to primary cilia in *Sey*/*Sey* show a reduction of more then 80 % (WT: 1 ± 0.26; *Sey*/*Sey*: 0.17 ± 0.13; * = $p<0.05$; $p = 0.03$). **h**, **i** Analysis of WT and *Sey*/*Sey* E15.5 cortex by IHC using antibodies against γ-Tubulin and ACIII show a significant loss of primary cilia at the ventricular surface in *Pax6* LOF brains. WT: 1 ± 0.06; *Sey*/*Sey*: 0.51 ± 0.09; ** = $p<0.01$; $p = 0.005$; $n = 3$; *bars* 10 µm)

Emx1Cre transgenic line [51], specifically to *Emx1-Cre*$^{+/-}$*;Pax6*$^{fl/fl}$ males [18]. Twenty-four hours after in utero electroporation at E13.5 with *Kaede-centrin1* plasmid, the brains were isolated, thick sectioned, and after photo conversion of the Kaede fluorescent protein, organotypic culturing of the brain sections was carried out for additional 48 h. During this time, the electroporated RGCs undergo 2 mitotic cycles, permitting the visualization of the mother centriole (in red) and the daughter centriole (in green) fluorescence via IHC [42, 52]. Quantitative analysis revealed that in *Pax6cKO* cortex, the VZ (identified through a clear immunosignal for the progenitor marker Sox2) contained significantly lower number of mother centrosomes compared to the control (Fig. 3a–f″), 70 % in the control and 40 % in the mutant (Fig. 3g, h respectively). Taken together, these results show a substantial reduction in the number of mature centrioles in the VZ, which become abundantly distributed in the CP in the Pax6 deficient brain (Fig. 3i).

Pax6 as a transcriptional regulator of *Odf2* gene

Given the phenotype of MC in *Sey*/*Sey* cortex described above, we hypothesized that the expression of the important determinant of centrosome maturation, Odf2/Cenexin, could be affected in *Pax6LOF*. The *Odf2* gene encodes the outer dense fibre 2 protein, located together with Ninein in the subdistal appendages of MC [39]. In the absence of Odf2, Ninein recruitment to the subdistal appendages and formation of primary cilia in murine F9 cells fail [47]. Ninein is involved in microtubule anchoring to the mother centriole, and in Ninein deficiency, cells containing the MC prematurely exit the mitotic cycle, leaving the VZ [42].

Whole-mount in situ hybridisation (ISH) analyses indicated a strong *Odf2* expression in the brain and spinal cord of E12.5 embryo brain, reminiscent to Pax6 expression, including the forebrain [53] (Fig. 4a). In addition, ISH at the peak of neurogenesis of the upper layer neuronal subtypes (E15.5), revealed that compared to the WT brain, the expression of *Odf2* in *Sey*/*Sey* cortex was significantly reduced (Fig. 4b, b′). To further support the observed reduction of *Odf2* expression, we performed quantitative real time PCR assays (RT-PCR), using cortices from E15.5 WT and *Sey*/*Sey* embryos. Consistent with the ISH data, the results revealed a strong down-regulation of *Odf2 e*xpression in E15.5 *Sey*/*Sey* cortex, compared to control (inhibition by 46.05 ± 6.24 %; $n = 3$) (Fig. 4c). Next we employed IHC to study the assembly of the mother centriole appendages in absence of Pax6, using IHC with antibody directed to Odf2 as a specific marker. Consistent with the ISH data, at E15.5 the expression of Odf2 protein in the mother centrosomes was strongly reduced in *Sey*/*Sey* compared to the control cortex (Fig. 4d, d′). In addition, immunostaining for Ninein, a protein mostly expressed at the subdistal appendages [47, 54], indicated a strong reduction of this mother centriole structural protein in the *Pax6* deficient cortex (Fig. 4e, e′).

As these findings were consistent with a direct regulation of *Odf2* by TF Pax6, we next performed a luciferase reporter gene assay in NIH3T3 cells using an expression plasmid in which firefly luciferase acted as a reporter under the control of the *Odf2* promoter [55]. Co-transfection of this together with a Pax6 expression plasmid (*CMV-Pax6*) revealed a slight activation (20 %) of the reporter (Fig. 4f). To assess Pax6 consensus-binding sites within 2.1 kb region of the *Odf2* promoter, we used MatInspector software analysis and identified three possible Pax6 binding sites (Fig. 5a). To validate the capacity of Pax6 to bind to those regulatory regions of *Odf2* we performed an electrophoretic mobility shift assay [56]. Incubation of radioactively labelled oligonucleotides for the predicted binding sites with Pax6 protein showed a strong binding to one of these sites (sequence 3 in Fig. 5b). To determine whether the binding was specific, the binding mixture was pre-incubated with an anti-Pax6 antibody (Fig. 5b). After electrophoresis, the protein-bound radiolabeled probes were supershifted, and thus contained the presence of a DNA-Pax6 protein antibody complex (line 6 in Fig. 5b). Together, these data indicate that in vitro Pax6 interacts specifically with the identified sequence 3 in the *Odf2* putative promoter.

To investigate whether Pax6 controls the expression of *Odf2* also in vivo we performed chromatin immunoprecipitation (ChIP) using cortical extracts from E12.5 embryos. As shown in Fig. 5c, DNA fragments containing

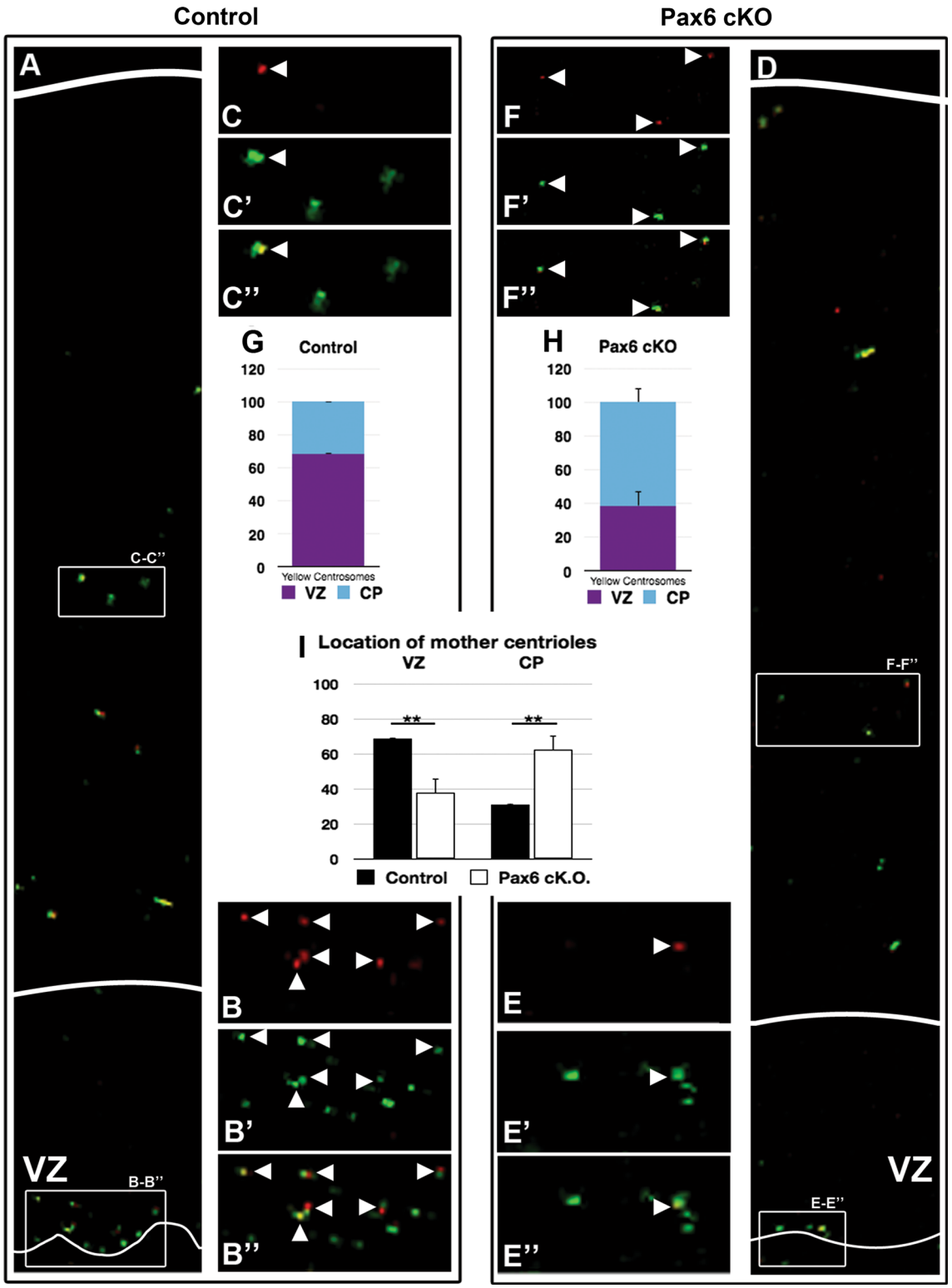

the sequence 3 of the putative *Odf2* promoter were precipitated by the anti-Pax6 antibody (but not by anti-GFP antibody) from the chromatin. In parallel we performed a ChIP assay on Chromatin from NIH3T3 cells following overexpression of Pax6 and this also indicated a specific Pax6/chromatin binding (data not shown).

Based on the direct regulation of *Odf2* by Pax6, altogether the above findings suggest that the subdistal

◀**Fig. 3** Abnormal behaviour of the mother centrosome containing the older (matured) centriole. Electroporation was done with *Kaede-Centrin1* plasmid of E13.5 embryo brains via in utero electroporation in pregnant mice (*Pax6*$^{fl/fl}$*Emx1cre*$^{+/-}$;*Pax6*$^{fl/fl}$) allowing conditional deletion of *Pax6* in RGCs [18], and after 24 h, a photoconversion on isolated brain sections was performed with UV light (350–400 nm). After additional culturing for 48 h, based on a specific immunofluorescence, quantification of the percentage of the differently aged mother (*green/red* or *yellow*; *arrowheads*) and daughter (*green*) centrioles was done. **a**–**c**, **g** In control cortex most of the mother centrioles (*red* and *green* signal) are located within VZ. Statistical analysis revealed around 70 % of mother centrosomes in the VZ only 30 % were located more basally (VZ: 68.69 ± 0.32; CP: 31.31 ± 0.32). **d**–**f″**, **h** In *Pax6LOF* cortex only around 40 % of mother centrosomes are located in VZ while around 60 % were located in CP (VZ: 37.65 ± 8.31 %; CP: 62.35 ± 8.31 %). **i** The diagram represents the results from the counting indicating that upon conditional deletion of Pax6 in RGCs, the Sox2^{+}VZ contains much less RGCs with mother centrioles. On the contrary, in *Pax6* deficiency, the CP contains higher number of mother centrioles (WT: VZ: 68.69 ± 0.32 %, CP: 31.31 ± 0.32 %; *Sey/Sey*: VZ: 37.65 ± 8.31 %, CP 62.35 ± 8.31 %; ** = p<0.01; p = 0.0074; control n = 3; *Pax6cKO* n = 4)

appendages of the mother centrioles in renewed RGCs are severely malformed, and are almost fully missing during late neurogenesis. Furthermore, this structural defect of MC clearly causes the loss of Ninein at the MC, as an indirect effect of *Pax6LOF*.

Loss of Odf2 causes premature exit of RGCs from mitosis

To study the role of Odf2 in cortical progenitors, we performed in vivo knock down of *Odf2* via in utero electroporation. Two effective *Odf2* short hairpin constructs were generated, SH3 and SH5 (Fig. 6b). Each of the short hairpin constructs or the control plasmid together with a GFP-expression plasmid was electroporated at E13.5 in WT embryo brains, and the cortices were analysed at E16.5. The performed IHC analysis (Fig. 6a–a″) revealed that after 72 h, normalized to the control, the *Odf2* knock down through SH3 and SH5 caused dramatic reduction in GFP^{+}/Pax6^{+} progenitors in the VZ, by 79.8 ± 6.18 and 73.67 ± 5.27 %, respectively (Fig. 6c), suggesting premature exit from mitosis and differentiation of RGPs. To analyse whether the loss of Pax6^{+} RGCs in the *Odf2* knock down cortex is due to premature cell cycle exit, we electroporated E13.5 embryo brains with either a control or a SH3 plasmid, together with a GFP-expression vector and, 24 h later, the pregnant mice were injected with BrdU solution (0.14 g/kg). After additional 24 h, the brains were dissected and analysed. To estimate the cell cycle exit index, IHC with antibodies against Ki67, BrdU and GFP was performed (Fig. 6f, f′). Ki67 vs. BrdU labelling indicates the relative proportion of cells exiting the cell cycle (Ki67^{-}/BrdU^{+}) and cells re-entering the cell cycle (Ki67^{+}/BrdU^{+}) after the last cell division. As expected, the analysis revealed that upon knockdown *Odf2* through SH3, considerably less cells were GFP^{+}/BrdU^{+}/Ki67^{+} (26.31 ± 2.1 %), and thus re-entered into mitosis as compared to the control (58.08 ± 3.04 %) (Fig. 6g).

To further validate that the loss of progenitors in the VZ is due to the reduced expression of *Odf2*, we subsequently performed in vivo rescue assays. Odf2- and empty GFP-expression plasmids were co-electroporated in E13.5 *Pax6cKO* embryos, and the cortex was analysed at E16.5 by IHC (Fig. 6d–d′). The results showed almost a three-fold (2.87 ± 0.7) increase in GFP^{+}/Sox2^{+} progenitors in the VZ compared to the cortex electroporated with empty vector and GFP-expression plasmid indicating maintenance of progenitor cells in the VZ in presence of high level of Odf2 (Fig. 6e).

Together these findings show that the appendage protein Odf2, which is regulated by TF Pax6 in RGCs, is an intrinsic factor for the RGC re-entry into the mitotic cycle, and is therefore significant for progenitor maintenance during cortical development.

Discussion

Transcription factor Pax6 is an intrinsic determinant for RGCs, exerting a number of important functions during cortical neurogenesis [15, 21, 24, 25, 27–29, 57–63]. Here, we report a novel role of TF Pax6 in centrosome assembly and maturation in RGCs.

To build up the layered structure of mammalian cortex, complex mechanisms including interkinetic nuclear migration [64] control the correct types of asymmetric divisions (direct and indirect) of the RGCs in the pallial apical VZ surface [3, 4, 6]. In *Pax*6 deficiency, as seen in the *Pax6*/*Sey*/*Sey* mutant, the interkinetic nuclear migration in RGCs is abnormal, including ectopic (basal) division of the apical progenitors and unstable centrosome positioning during the S to M phase of the cell cycle [31, 65]. Each centrosome consists of a pair of centrioles that has specific morphology and function [34, 66–68]. The mother centriole, which is generated at least one and a half cell cycles earlier than the daughter centriole, contains appendages that incorporate numerous distinct proteins including Odf2 [38, 39], and Ninein [37, 41].

The proposed role of the appendage protein Ninein is quite controversial. Asami et al. [30] found reduced expression of Ninein in *Sey/Sey* mice and a spindle disorientation after knock down of Ninein, while other authors showed premature exit from the mitotic cycle of RGCs, and affected interkinetic nuclear migration after Ninein knock down, due to a missing anchorage of microtubules to the centrosome [42, 69]. As shown by

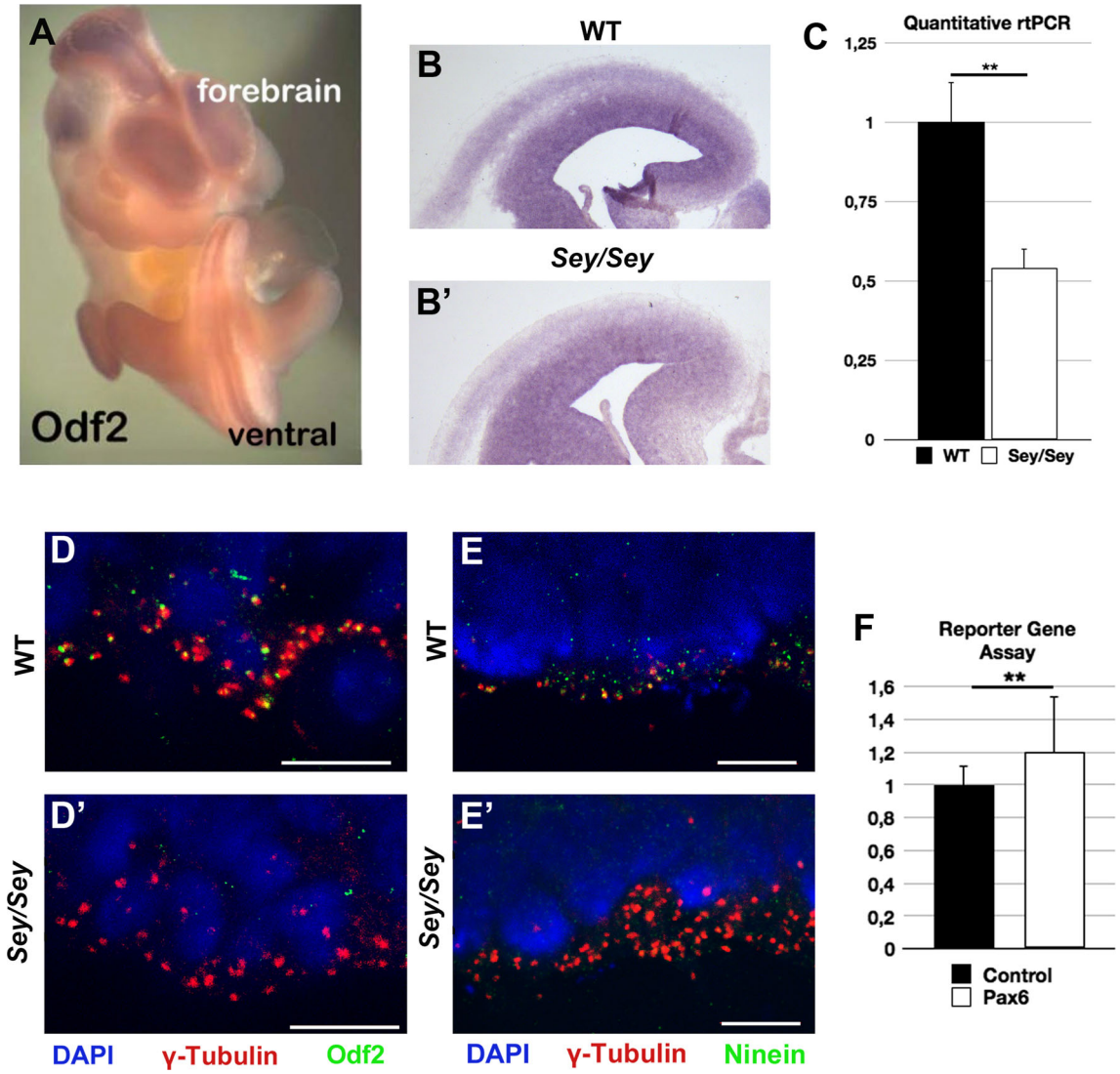

Fig. 4 The expression of mother centriole specific proteins Odf2 and Ninein are down regulated in Pax6 deficient cortex. **a** Whole-mount ISH shows a strong expression of *Odf2* mRNA in the forebrain. **b**–**b**′ ISH on cross brain sections shows suppression of *Odf2* expression at E15.5 in the *Pax6* mutant cortex. **c** The diagram illustrates the relative expression level of *Odf2* transcripts using quantitative RT-PCR analysis in *Pax6LOF* cortex compared to WT *:<0.05 ($p = 0.0057$); $n = 3$. **d**–**d**′ IHC with antibody for Odf2 (*green*) on cross E15.5 WT (**d**) and *Sey*/*Sey* (**d**′) sections reveals absence of appendages in MC in *Pax6LOF*. **e**–**e**′ IHC with antibody for Ninein (*green*) shows reduced expression at the centrioles (γ-Tubulin+/in *red*) in the *Sey*/*Sey* cortex (**e**′) E15.5 (*bars* 10 μm). **f** Co-transfection of NIH3T3 cells in vitro with expression plasmids for *Odf2* promoter in front of firefly luciferase reporter sequence together *CMV-Pax6* expression plasmid, causes activation of *Odf2-promoter-luciferase* activity, suggesting a genetic interplay between the two genes

Wang et al. [42] after mitosis, the centrosomes are asymmetrically inherited with a mature MC, kept within the renewed RGC and a younger DC, and included in the differentiating cells. Knock down of Ninein hampers this effect, resulting in premature exit from the mitotic cycle [42], which is similar to the effect observed here in *Sey*/*Sey* mice [18, 24]. Surprisingly, up until now no evidence has been presented showing Ninein is a direct downstream target of Pax6 [69] suggesting that the loss of Ninein from the mother centrioles appendages might be a secondary effect.

In this study, we found that TF Pax6 directly regulates the expression of *Odf2,* and thereby the production of a structural protein that is an essential compartment of the mother centriole subdistal appendages, working structurally upstream of the appendage protein Ninein [54]. We were able to show a loss of Odf2 at the centrosome additionally to the loss of Ninein in the *Pax6LOF* phenotype. An earlier publication proposed a direct relationship between the loss of Odf2 and the loss of Ninein at the subdistal appendages suggesting an important role of Odf2 for Ninein recruitment to the subdistal appendages [47]. As shown here, the knock

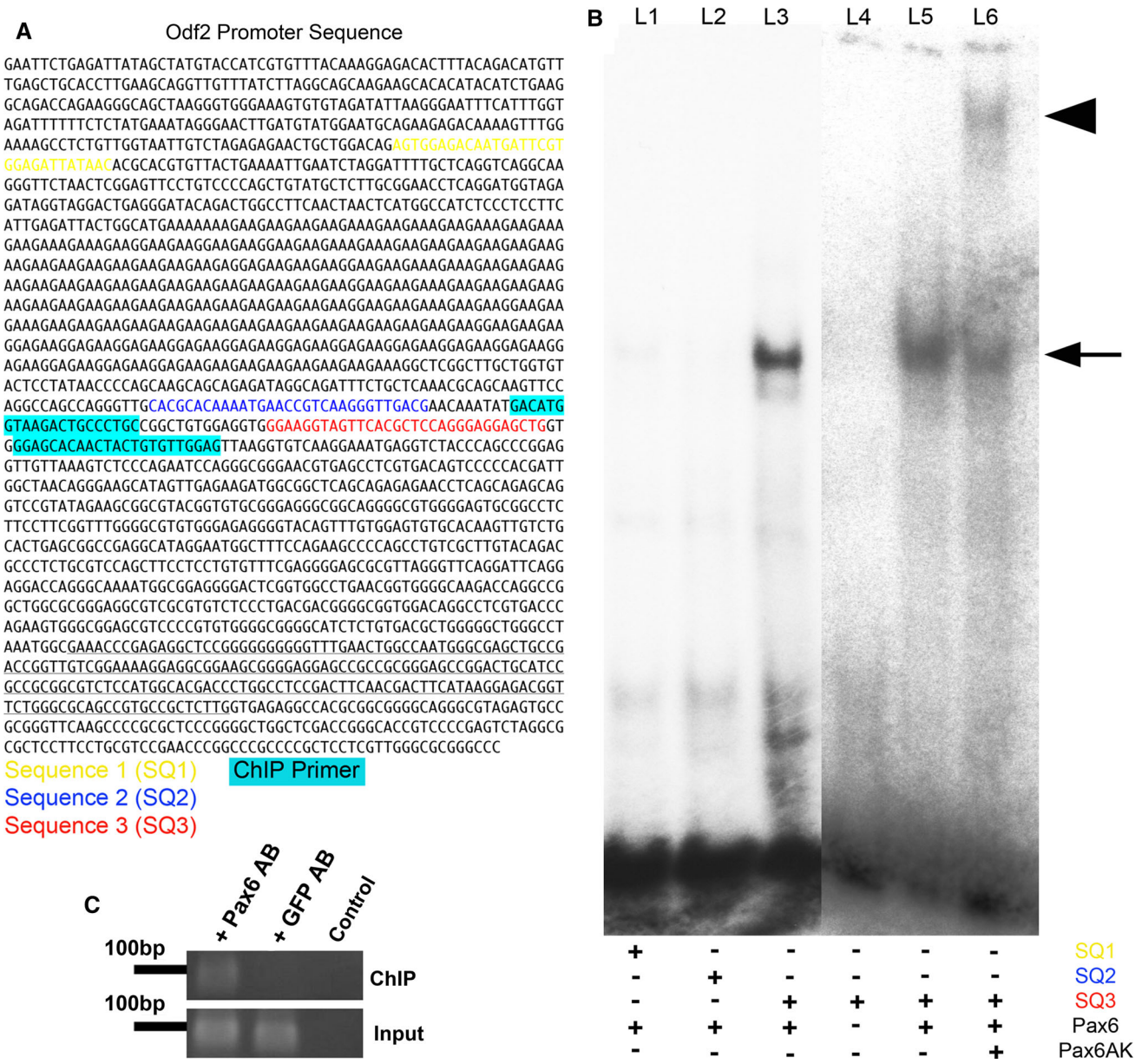

Fig. 5 *Odf2* is a downstream target of TF Pax6 in cortical progenitors. **a** Three sequence (SQ1, SQ2, SQ3, *coloured*) in the *Odf2* promoter contain consensus Pax6 binding sites. **b** Electrophoretic mobility shift assays performed with in vitro translated Pax6 protein and P^{32}-labelled oligonucleotides for the identified 3 consensus Pax6 binding sites (in lane 1, SQ1; in lane 2, SQ2; in lane 3, SQ3) in the *Odf2* promoter show that Pax6 binds strongly to one (SQ3, lane 3) of these sites. Pre-incubation of the binding mixture with a Pax6 antibody shows a supershift (lane 6, *arrowhead*) of the protein-bound radiolabeled probe, confirming the specificity of the DNA-Pax6protein-Pax6 antibody complex. Controls in lane 4 and lane 5 show absence of shifting when the binding mixture contains only SQ3 or SQ3 and translated Pax6 protein, respectively. **c** In a ChIP Pax6 antibodies precipitated the Pax6 binding sequence within the *Odf2* promoter

down of Odf2/Cenexin caused a loss of RGCs as a result of premature exit of RGCs from mitotic cycle in *Pax6LOF*. Furthermore, we found that Odf2/Cenexin overexpression in Pax6-deficient background was able to rescue the premature exit of RGCs from mitotic cycle, supporting the idea that the loss of Odf2 (and not of Ninein itself) is the reason for the defective re-entry of RGCs into the mitotic cycle in the *Sey*/*Sey* mutant cortex. We also found that in lack of Pax6, the compromised centrosome maturation is accompanied by defect in asymmetric partitioning of the two centrosomes. Thus, our results reveal a new molecular mechanism involved in progenitor maintenance in the VZ via *Pax6* dependent control of the expression of appendage-specific protein Odf2.

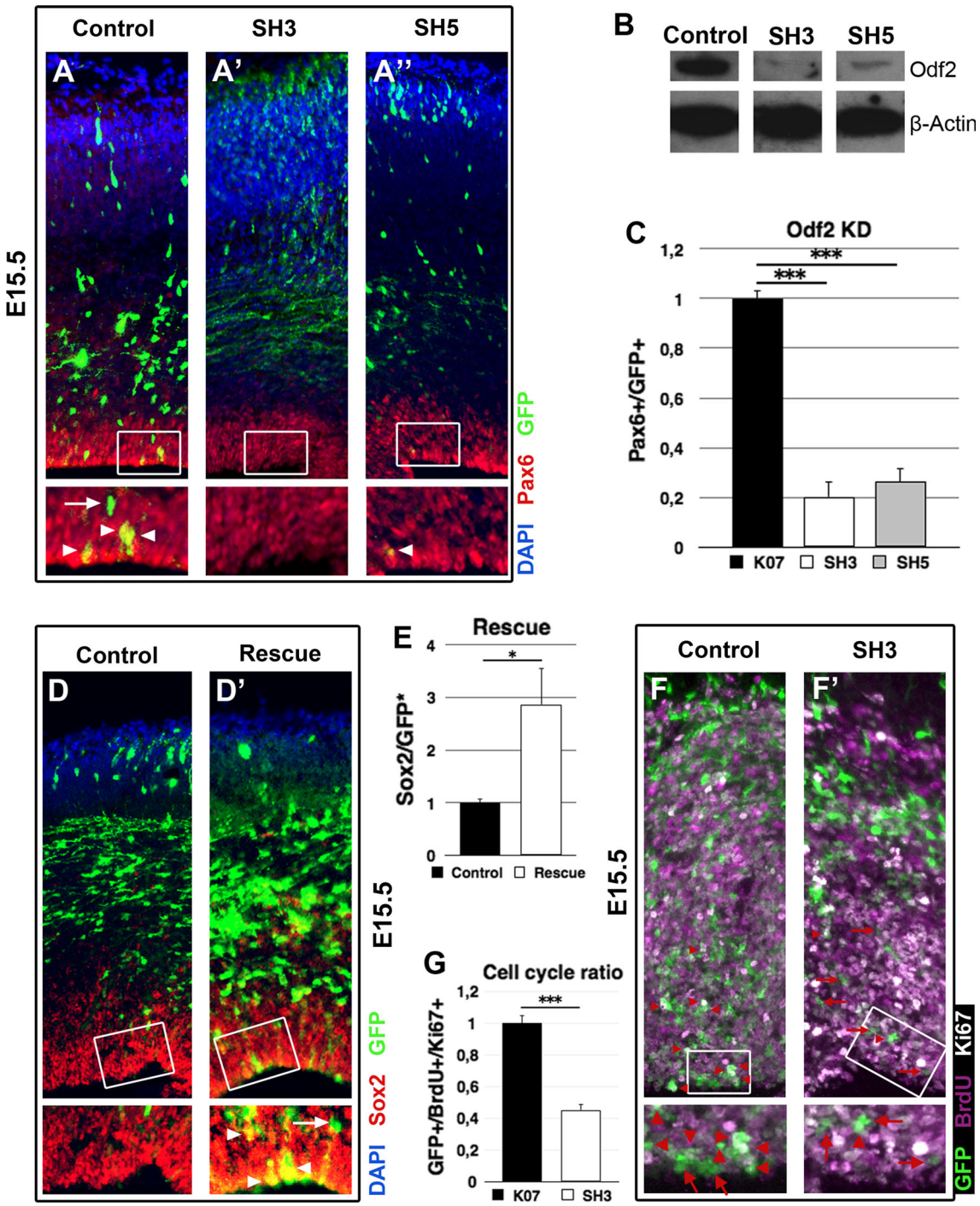

In accordance with findings of Ishikawa et al. [47], that Odf2 is essential for the primary cilia formation in F9 cells, we were able to demonstrate that also in *Sey*/*Sey* embryos less centrioles were connected to primary cilia and less RGCs were able to form a primary cilia into the ventricle (Fig. 2). This defect is possibly caused by a mis-localisation of the centrosome, as shown by Tamai et al. [31], because of missing anchorage of the basal body to the plasma membrane. Cilia have a critical role in signal transduction controlled by SHH and WNT [46, 70, 71], and cilia malformation in *Pax6LOF* as shown here, could be related to at least two of the abnormalities in the *Pax6* deficient cortex: enlargement of Wnt3a expression domain in the E10.5 telencephalic primordium [72] and defective dorsoventral molecular patterning of forebrain [37–59, 61].

In conclusion, in this report we have shown a new link between centrosome misbehaviour and TF Pax6. By regulating directly the expression of *Odf2, Pax6* controls

◀**Fig. 6** *Odf2* knock down in developing cortex in vivo causes premature cell cycle exit. **a**–**a**″ Forced expression of individual Odf2-sh plasmid (SH3/SH5), showing a strong capacity to reduce Odf2 level in vitro, as demonstrated in (**b**) or control plasmid together with GFP-plasmid to mark the electroporated cells was done in E13.5 embryo brains via in utero electroporation and analysis was performed at E16.5. **a** IHC with RGC marker Pax6 indicates a severe diminishing of RGC number (GFP+/Pax6+/*yellow*, pointed by *arrowheads*) upon Odf2 knock down with both SH3 (**A**′) and SH5 (**A**″). **c** Counting indicated that normalized to the control, Odf2 knock down causes a reduction of the RGC number by approximately 80 % with SH3 and with 75 % with SH5 (control: 1 ± 0.03; $n = 3$; SH3: 0.2 ± 0.06; *** = $p < 0.001$; $p = 0.0005$; $n = 3$; SH5: 0.26 ± 0.05; $p = 0.0002$; $n = 3$). The *arrow* in **a** shows Pax6 negative cell leaving VZ. **d**, **d**′ Overexpression of *Odf2* rescues the Odf2 knock down phenotype in *Pax6LOF* cortex. *Pax6cKO* embryos were electroporated with an Odf2 expression plasmid (**d**′) or a control plasmid (**d**) at E13.5 and analysed at E16.5. **e** After *Odf2* overexpression the number of $GFP^+/Sox2^+$ was almost three times higher then after control plasmid expression (control: 1 ± 0.07; $n = 4$; Odf2 over expression: 2.87 ± 0.70; $n = 4$; * = $p<0.05$; $p = 0.01$). **f**, **f**′, **g** 24 h after the performed in utero electroporation with either SH3 (**f**′) or control plasmid (**f**), BrdU pulse labelling for 24 h was done, and IHC analysis with antibodies for GFP, BrdU and Ki67 was performed. *Red arrows* indicate $GFP^+/BrdU^+/Ki67^+$ cells, while *red arrowheads*: $GFP^+/BrdU^+/Ki67^-$ cells. **g** Quantification of the index for cell cycle exit indicates a premature exit of RGCs from mitotic cycle after knock down of *Odf2* (in the control, dividing RGC: 1 ± 0.05; $n = 3$; after SH3-Odf2KD: 0.45 ± 0.04; $n = 3$; ***: $p < 0.005$ ($p = 0.00051$)

centriole maturation in apical progenitors and consequently the re-entry of RGCs in the mitotic cycle.

Materials and methods

Animals

Small eye (allele *Sey*) $Pax6^{fl/fl}$ and $Emx1^{Ires-Cre}$ were maintained in a C57BL6/J background. *Sey*/+ male and female were crossed to produce *Sey/Sey* mice. +/+ embryos from the same litter were used as control. CD1 mice were used for in utero electroporation of short hairpin constructs and control constructs. For in utero electroporation of Kaede-Centrin1 we used transgenic mice with a floxed *Pax6* allele [50] and the $Emx1Cre^{+/-}$ [51] mouse lines. We crossed female $Pax6^{fl/fl}$ with male $Pax6^{fl/fl}$; $Emx1^{+/-}$ to produce $Pax6^{fl/fl}$;l$Emx1Cre^{+/-}$ embryos named *Pax6cKO*. $Pax6^{fl/fl}$ embryos were used as control. Animals were handled in accordance with the German Animal Protection Law and with the permission of the Bezirksregierung Braunschweig.

In utero electroporation

In utero electroporation was performed using 2.5 µg/µl endotoxin-free DNA plasmids prepared using EndoFree Plasmid (Qiagen). An eGFP plasmid was co-injected with SH3, SH5 or control plasmid at a concentration of 1:1. E13.5 or E15.5 CD1 mice were anesthetized by intraperitoneal injection of Ketamine/Xylazine (100/10 mixture, 0.1 mg per gram body weight). The uterine horns were carefully exposed through the incision using O-ringed forceps and humidified gauze pads. Plasmids were injected with 0.05 % Fast Green (Sigma) into the telecephalic lateral ventricles of embryos using pulled glass capillaries. Five electrical pulses were applied at 30–35 V using platinum tweezer electrodes (CUY650P3, BEX Co., Ltd.). The uterine horns were then replaced in the abdominal cavity and skins were sutured using a surgical needle and thread. Three days after electroporation, pregnant mice were killed and embryos were processed for histological analysis.

Photoswitch and culture of Kaede-Centrin1 electroporated brains slides

Brains were electroporated with Kaede-Centrin1 plasmid as described. After 24 h, mice were killed and embryonic brains were embedded in 2 % low melting agarose in EBSS (Gibco) and cut in 400 µm slices with a vibratom. Slices were cultured on Millicell cell culture inserts (Millipore) with brain slice culture medium (50 % EBM (Gibco); 25 % HBSS (Gibco); 5 % FBS; 1 % 100× N2 supplement (Gibco); 1 % 100× Penicillin/Streptomycin (Gibco); 1 % 100× Glutamin (Gibco); 0.66 % D-(+)-glucose (Sigma). Before incubation slides were exposed to UV light (350–400 nm) for 5 s. After 2 days of incubation in a humidified incubator (37 °C; 5 % CO_2) slides were fixed with 4 % PFA and embedded in tissue freezing medium (Jung).

Identification of Pax6 binding sites in the Odf2 promoter

To identify potential binding sites within a 2,1-kb region of the mouse *Odf2* promoter we searched for the reported Pax6 consensus-binding site [73] with MatInspector software.

Determination of Pax6 DNA binding

Electrophoretic mobility shift assay (EMSA) has been used. PAX6 proteins were expressed using the TNT in vitro transcription and translation system (Promega), according to manufacturer's instructions. Double-stranded oligonucleotides were end-labelled using polynucleotide kinase and γ-^{P32}ATP. The binding reaction was performed for 1 h on ice in binding buffer (25 mM HEPES pH7.4, 10 % glycerol, 75 mM NaCl, 0.25 mM EDTA, 1 mM DTT, 0.1 % Nonidet P-40, 1 mM $MgCl_2$, protease inhibitor cocktail) containing 0.5 µg poly-dI-dC, double-stranded oligonucleotides (with radial activity at 35,000 cpm) and

10 µl of in vitro-translated Pax6 protein. For antibody supershift analyses, 0.5 µl of Pax6 polyclonal rabbit antibody (Covance) was added and samples were incubated for additional 15 min. Samples were loaded onto 4 % TAE polyacrylamide gels and electrophoresed at 10 V/cm to resolve complexes. Gels were dried and processed for autoradiography.

Chromatin immunoprecipitation (ChIP) assay

Chromatin was extracted from E12.5 cortices. ChIP assays were performed according to manufacture's instruction (Chromatin Immunoprecipitation (ChIP) Assay Kit, Millipore) using polyclonal Pax6 antibodies (rabbit, Covance) to immunoprecipitate Pax6-binding chromatin fragments, with pre-immune serum and polyclonal GFP antibodies (Abcam) as immunoprecipitation controls (10 µg antibody per immunoprecipitation).

Generation and characterization of *Odf2* RNAi vector

Oligonucleotides were selected, synthesized commercially, and cloned into the pSilencer-2.0 vector (Ambion), which places shRNA expression under the control of the U6 promoter. In this study 8 Odf2 shRNA plasmids (SH1-8) and a control plasmid lacking homology with any known mRNA were used. All shRNA plasmids were co-transfected with HA-Odf2 into NIH3T3 cells and cultured for 2 days. Western blotting was used to analyse the efficiency of knockdown by shRNA(s). Therefore NIH3T3 cells were harvested with 0.25 % Trypsin (GIBCO) and quantified. Similar amounts of cell lysate were applied on SDS-PAGE and probed with antibody against HA (rat; 1:500; Roche). For loading control antibody for β-Actin was used. Two shRNAs (SH3 and SH5) with the sequence 5′-AAGAA CTCCTCCAGGAGATAC-3′ (SH3) and 5′-AATAAACA GCTGAGTCAGAAG-3′ (SH5) were found to result in the most efficient knock down Odf2 expression and were used in all subsequent experiments.

Tissue preparation

Isolated brains were fixated in 4 % paraformaldehyde in PBS for 1.5 h (E13.5), 2 h (E15.5) or 2.5 h (E16.5), respectively, at 4 °C. Tissues were rinsed in PBS and equilibrated overnight at 25 % sucrose/PBS at 4 °C for cryoprotection. Then tissue was frozen in Tissue freezing medium (Jung).

Immunohistochemistry

Brain Sections (16 µm) were blocked for 1 h in blocking solution (10 % normal goat serum in PBT). Primary antibodies were incubated over night at 4 °C in blocking solution. After 3 times washing in PBS, sections were incubated with secondary antibodies (Invitrogen) for 2 h at room temperature, washed again and mounted with Vectashild mounting medium (Vector Labs) containing 4′,6-diamidino-2-phenylindole (DAPI). We used the following primary antibodies/dilutions: ACIII (rabbit; 1:500), BrdU (rat; 1:200; Abcam), GFP (chicken; 1:500; Abcam), Ki67 (rabbit; 1:100; Vector Labs), Ninein (rabbit; 1:500; Abcam), Odf2 (rabbit; 1:50), Pax6 (rabbit; 1:300; Covance/mouse; 1:200; DSHB), Sox2 (rabbit; 1:200; Millipore). The anti-BrdU antibody was visualized after pretreatment of tissues in 2 N HCl at 37 °C for 30 min.

In situ hybridisation

Non-radioactive in situ hybridisation was carried out on Cryo-brain-sections (16 µm) according to Muhlfriedel et al. [74].

Electron microscopy of E15.5 embryonic cortex

Cortex hemispheres of E15.5 WT and *Pax6/Small* eye homozygous (*Sey/Sey*) embryos [20] were dissected and prepared for Epon embedding. Semi-thin cuttings were used for trimming. Ultra thin sections were analysed by transmission electron microscopy.

Cell culture

NIH3T3 cells and HEK-293 cells were maintained and cultured in DMEM medium plus 10 % FCS. Cells were transfected using Transfectin (BioRad) according to supplier's guidelines. For the luciferase assay, cells were transfected with *Odf2-promoter-luciferase* construct alone or together with Pax6 expression plasmid (*CMV-Pax6*). For quantitative analysis of Odf2 cells were transfected with *HA-Odf2* together with control plasmid or SH-construct containing plasmid, respectively.

Luciferase assay

Cells were lysed and assayed for Luciferase activity according to the assay manufacturer's instructions (Promega).

qPCR analysis

Total RNA was extracted from cortex cells by peqGOLD RNAPureTM and digested with RQ1 DNase. cDNA was generated from 0.5 µg of total RNA using RevertAidTM H Minus First Strand cDNA Synthesis Kit (Fermentas) and oligo(dT)18 primer. Real time PCR was performed on

iCycler IQ PCR System (BioRad) using cloned *Odf2* and *Hprt* fragments, respectively, as standard fort quantification. The specificity of the SYBR Green assay was verified by melting curve analysis.

Statistical analysis

Results are presented as mean ± standard deviation (SD). The number of experiments is indicated in the figure legends. Statistical differences were evaluated using Student's *t* test.

Acknowledgments The authors thank Prof. Dr. med Nicolai Miosge for technical and knowledge support regarding electron microscopy. Thanks are also due to Silke Schlott and Martina Daniel for excellent technical assistance. We thank T. Schweizer for proofreading. Marco A. Tylkowski was funded through Cluster of Excellence and DFG Research Center Nanoscale Microscopy and Molecular Physiology of the Brain.

References

1. Caviness VS Jr, Takahashi T (1995) Proliferative events in the cerebral ventricular zone. Brain Dev 17(3):159–163
2. Caviness VS Jr, Takahashi T, Nowakowski RS (1995) Numbers, time and neocortical neuronogenesis: a general developmental and evolutionary model. Trends Neurosci 18(9):379–383
3. Gotz M, Huttner WB (2005) The cell biology of neurogenesis. Nat Rev Mol Cell Biol 6(10):777–788. doi:10.1038/nrm1739
4. Kriegstein A, Noctor S, Martinez-Cerdeno V (2006) Patterns of neural stem and progenitor cell division may underlie evolutionary cortical expansion. Nat Rev Neurosci 7(11):883–890. doi:10.1038/nrn2008
5. Malatesta P, Hartfuss E, Gotz M (2000) Isolation of radial glial cells by fluorescent-activated cell sorting reveals a neuronal lineage. Development 127(24):5253–5263
6. Miyata T (2007) Asymmetric cell division during brain morphogenesis. Prog Mol Subcell Biol 45:121–142
7. Noctor SC, Flint AC, Weissman TA, Dammerman RS, Kriegstein AR (2001) Neurons derived from radial glial cells establish radial units in neocortex. Nature 409(6821):714–720. doi:10.1038/35055553
8. Rakic P (2009) Evolution of the neocortex: a perspective from developmental biology. Nat Rev Neurosci 10(10):724–735. doi:10.1038/nrn2719
9. McConnell SK, Kaznowski CE (1991) Cell cycle dependence of laminar determination in developing neocortex. Science 254(5029):282–285
10. Angevine JB Jr, Sidman RL (1961) Autoradiographic study of cell migration during histogenesis of cerebral cortex in the mouse. Nature 192:766–768
11. Rakic P, Stensas LJ, Sayre E, Sidman RL (1974) Computer-aided three-dimensional reconstruction and quantitative analysis of cells from serial electron microscopic montages of foetal monkey brain. Nature 250(461):31–34
12. Haubensak W, Attardo A, Denk W, Huttner WB (2004) Neurons arise in the basal neuroepithelium of the early mammalian telencephalon: a major site of neurogenesis. Proc Natl Acad Sci USA 101(9):3196–3201. doi:10.1073/pnas.0308600100
13. Lukaszewicz A, Savatier P, Cortay V, Giroud P, Huissoud C, Berland M, Kennedy H, Dehay C (2005) G1 phase regulation, area-specific cell cycle control, and cytoarchitectonics in the primate cortex. Neuron 47(3):353–364. doi:10.1016/j.neuron.2005.06.032
14. Noctor SC, Martinez-Cerdeno V, Ivic L, Kriegstein AR (2004) Cortical neurons arise in symmetric and asymmetric division zones and migrate through specific phases. Nat Neurosci 7(2):136–144. doi:10.1038/nn1172
15. Bishop KM, Goudreau G, O'Leary DD (2000) Regulation of area identity in the mammalian neocortex by Emx2 and Pax6. Science 288(5464):344–349
16. Georgala PA, Carr CB, Price DJ (2011) The role of Pax6 in forebrain development. Dev Neurobiol 71(8):690–709. doi:10.1002/dneu.20895
17. Hevner RF, Shi L, Justice N, Hsueh Y, Sheng M, Smiga S, Bulfone A, Goffinet AM, Campagnoni AT, Rubenstein JL (2001) Tbr1 regulates differentiation of the preplate and layer 6. Neuron 29(2):353–366
18. Tuoc TC, Radyushkin K, Tonchev AB, Pinon MC, Ashery-Padan R, Molnar Z, Davidoff MS, Stoykova A (2009) Selective cortical layering abnormalities and behavioral deficits in cortex-specific Pax6 knock-out mice. J Neurosci 29(26):8335–8349. doi:10.1523/JNEUROSCI.5669-08.2009
19. Zembrzycki A, Chou SJ, Ashery-Padan R, Stoykova A, O'Leary DD (2013) Sensory cortex limits cortical maps and drives top-down plasticity in thalamocortical circuits. Nat Neurosci 16(8):1060–1067. doi:10.1038/nn.3454
20. Hill RE, Favor J, Hogan BL, Ton CC, Saunders GF, Hanson IM, Prosser J, Jordan T, Hastie ND, van Heyningen V (1991) Mouse small eye results from mutations in a paired-like homeobox-containing gene. Nature 354(6354):522–525. doi:10.1038/354522a0
21. Heins N, Malatesta P, Cecconi F, Nakafuku M, Tucker KL, Hack MA, Chapouton P, Barde YA, Gotz M (2002) Glial cells generate neurons: the role of the transcription factor Pax6. Nat Neurosci 5(4):308–315. doi:10.1038/nn828
22. Caric D, Gooday D, Hill RE, McConnell SK, Price DJ (1997) Determination of the migratory capacity of embryonic cortical cells lacking the transcription factor Pax-6. Development 124(24):5087–5096
23. Georgala PA, Manuel M, Price DJ (2011) The generation of superficial cortical layers is regulated by levels of the transcription factor Pax6. Cereb Cortex 21(1):81–94. doi:10.1093/cercor/bhq061
24. Quinn JC, Molinek M, Martynoga BS, Zaki PA, Faedo A, Bulfone A, Hevner RF, West JD, Price DJ (2007) Pax6 controls cerebral cortical cell number by regulating exit from the cell cycle and specifies cortical cell identity by a cell autonomous mechanism. Dev Biol 302(1):50–65. doi:10.1016/j.ydbio.2006.08.035
25. Sansom SN, Livesey FJ (2009) Gradients in the brain: the control of the development of form and function in the cerebral cortex. Cold Spring Harb Perspect Biol 1(2):a002519. doi:10.1101/cshperspect.a002519
26. Schmahl W, Knoedlseder M, Favor J, Davidson D (1993) Defects of neuronal migration and the pathogenesis of cortical malformations are associated with Small eye (Sey) in the mouse, a point mutation at the Pax-6-locus. Acta Neuropathol 86(2):126–135
27. Stoykova A, Fritsch R, Walther C, Gruss P (1996) Forebrain patterning defects in Small eye mutant mice. Development 122(11):3453–3465
28. Tarabykin V, Stoykova A, Usman N, Gruss P (2001) Cortical upper layer neurons derive from the subventricular zone as indicated by Svet1 gene expression. Development 128(11):1983–1993
29. Gotz M, Stoykova A, Gruss P (1998) Pax6 controls radial glia differentiation in the cerebral cortex. Neuron 21(5):1031–1044

30. Asami M, Pilz GA, Ninkovic J, Godinho L, Schroeder T, Huttner WB, Gotz M (2011) The role of Pax6 in regulating the orientation and mode of cell division of progenitors in the mouse cerebral cortex. Development 138(23):5067–5078. doi:10.1242/dev.074591
31. Tamai H, Shinohara H, Miyata T, Saito K, Nishizawa Y, Nomura T, Osumi N (2007) Pax6 transcription factor is required for the interkinetic nuclear movement of neuroepithelial cells. Genes Cells 12(9):983–996. doi:10.1111/j.1365-2443.2007.01113.x
32. Tuoc TC, Stoykova A (2008) Er81 is a downstream target of Pax6 in cortical progenitors. BMC Dev Biol 8:23. doi:10.1186/1471-213X-8-23
33. Kosodo Y (2012) Interkinetic nuclear migration: beyond a hallmark of neurogenesis. Cell Mol Life Sci 69(16):2727–2738. doi:10.1007/s00018-012-0952-2
34. Bornens M (2002) Centrosome composition and microtubule anchoring mechanisms. Curr Opin Cell Biol 14(1):25–34
35. Higginbotham HR, Gleeson JG (2007) The centrosome in neuronal development. Trends Neurosci 30(6):276–283. doi:10.1016/j.tins.2007.04.001
36. Tsou MF, Stearns T (2006) Mechanism limiting centrosome duplication to once per cell cycle. Nature 442(7105):947–951. doi:10.1038/nature04985
37. Bouckson-Castaing V, Moudjou M, Ferguson DJ, Mucklow S, Belkaid Y, Milon G, Crocker PR (1996) Molecular characterisation of ninein, a new coiled-coil protein of the centrosome. J Cell Sci 109(Pt 1):179–190
38. Lange BM, Gull K (1995) A molecular marker for centriole maturation in the mammalian cell cycle. J Cell Biol 130(4):919–927
39. Nakagawa Y, Yamane Y, Okanoue T, Tsukita S, Tsukita S (2001) Outer dense fiber 2 is a widespread centrosome scaffold component preferentially associated with mother centrioles: its identification from isolated centrosomes. Mol Biol Cell 12(6):1687–1697
40. Ou YY, Mack GJ, Zhang M, Rattner JB (2002) CEP110 and ninein are located in a specific domain of the centrosome associated with centrosome maturation. J Cell Sci 115(Pt 9):1825–1835
41. Piel M, Meyer P, Khodjakov A, Rieder CL, Bornens M (2000) The respective contributions of the mother and daughter centrioles to centrosome activity and behavior in vertebrate cells. J Cell Biol 149(2):317–330
42. Wang X, Tsai JW, Imai JH, Lian WN, Vallee RB, Shi SH (2009) Asymmetric centrosome inheritance maintains neural progenitors in the neocortex. Nature 461(7266):947–955. doi:10.1038/nature08435
43. Hoyer-Fender S (2010) Centriole maturation and transformation to basal body. Semin Cell Dev Biol 21(2):142–147. doi:10.1016/j.semcdb.2009.07.002
44. Kobayashi T, Dynlacht BD (2011) Regulating the transition from centriole to basal body. J Cell Biol 193(3):435–444. doi:10.1083/jcb.201101005
45. Willaredt MA, Hasenpusch-Theil K, Gardner HA, Kitanovic I, Hirschfeld-Warneken VC, Gojak CP, Gorgas K, Bradford CL, Spatz J, Wolfl S, Theil T, Tucker KL (2008) A crucial role for primary cilia in cortical morphogenesis. J Neurosci 28(48):12887–12900. doi:10.1523/JNEUROSCI.2084-08.2008
46. Willaredt MA, Tasouri E, Tucker KL (2012) Primary cilia and forebrain development. Mech Dev. doi:10.1016/j.mod.2012.10.003
47. Ishikawa H, Kubo A, Tsukita S (2005) Odf2-deficient mother centrioles lack distal/subdistal appendages and the ability to generate primary cilia. Nat Cell Biol 7(5):517–524. doi:10.1038/ncb1251
48. Tong CK, Han YG, Shah JK, Obernier K, Guinto CD, Alvarez-Buylla A (2014) Primary cilia are required in a unique subpopulation of neural progenitors. Proc Natl Acad Sci USA. doi:10.1073/pnas.1321425111
49. Imai JH, Wang X, Shi SH (2010) Kaede-centrin1 labeling of mother and daughter centrosomes in mammalian neocortical neural progenitors. Curr Protoc Stem Cell Biol 5:5A. doi:10.1002/9780470151808.sc05a05s15
50. Ashery-Padan R, Marquardt T, Zhou X, Gruss P (2000) Pax6 activity in the lens primordium is required for lens formation and for correct placement of a single retina in the eye. Genes Dev 14(21):2701–2711
51. Gorski JA, Talley T, Qiu M, Puelles L, Rubenstein JL, Jones KR (2002) Cortical excitatory neurons and glia, but not GABAergic neurons, are produced in the Emx1-expressing lineage. J Neurosci 22(15):6309–6314. doi:10.1016/b0-12-227210-2/00147-3
52. Cai L, Hayes NL, Nowakowski RS (1997) Local homogeneity of cell cycle length in developing mouse cortex. J Neurosci 17(6):2079–2087
53. Walther C, Gruss P (1991) Pax-6, a murine paired box gene, is expressed in the developing CNS. Development 113(4):1435–1449
54. Ibi M, Zou P, Inoko A, Shiromizu T, Matsuyama M, Hayashi Y, Enomoto M, Mori D, Hirotsune S, Kiyono T, Tsukita S, Goto H, Inagaki M (2011) Trichoplein controls microtubule anchoring at the centrosome by binding to Odf2 and ninein. J Cell Sci 124(Pt 6):857–864. doi:10.1242/jcs.075705
55. Pletz N, Medack A, Riess EM, Yang K, Kazerouni ZB, Huber D (1833) Hoyer-Fender S (2013) Transcriptional activation of Odf2/Cenexin by cell cycle arrest and the stress activated signaling pathway (JNK pathway). Biochim Biophys Acta 6:1338–1346. doi:10.1016/j.bbamcr.2013.02.023
56. Baumer N, Marquardt T, Stoykova A, Spieler D, Treichel D, Ashery-Padan R, Gruss P (2003) Retinal pigmented epithelium determination requires the redundant activities of Pax2 and Pax6. Development 130(13):2903–2915
57. Stoykova A, Treichel D, Hallonet M, Gruss P (2000) Pax6 modulates the dorsoventral patterning of the mammalian telencephalon. J Neurosci 20(21):8042–8050
58. Yun K, Potter S, Rubenstein JL (2001) Gsh2 and Pax6 play complementary roles in dorsoventral patterning of the mammalian telencephalon. Development 128(2):193–205
59. Toresson H, Potter SS, Campbell K (2000) Genetic control of dorsal-ventral identity in the telencephalon: opposing roles for Pax6 and Gsh2. Development 127(20):4361–4371
60. Warren N, Caric D, Pratt T, Clausen JA, Asavaritikrai P, Mason JO, Hill RE, Price DJ (1999) The transcription factor, Pax6, is required for cell proliferation and differentiation in the developing cerebral cortex. Cereb Cortex 9(6):627–635
61. Kroll TT, O'Leary DD (2005) Ventralized dorsal telencephalic progenitors in Pax6 mutant mice generate GABA interneurons of a lateral ganglionic eminence fate. Proc Natl Acad Sci USA 102(20):7374–7379. doi:10.1073/pnas.0500819102
62. Estivill-Torrus G, Pearson H, van Heyningen V, Price DJ, Rashbass P (2002) Pax6 is required to regulate the cell cycle and the rate of progression from symmetrical to asymmetrical division in mammalian cortical progenitors. Development 129(2):455–466
63. Schuurmans C, Armant O, Nieto M, Stenman JM, Britz O, Klenin N, Brown C, Langevin LM, Seibt J, Tang H, Cunningham JM, Dyck R, Walsh C, Campbell K, Polleux F, Guillemot F (2004) Sequential phases of cortical specification involve Neurogenin-dependent and -independent pathways. EMBO J 23(14):2892–2902. doi:10.1038/sj.emboj.7600278
64. Messier PE, Auclair C (1973) Inhibition of nuclear migration in the absence of microtubules in the chick embryo. J Embryol Exp Morphol 30(3):661–671

65. Osumi N, Shinohara H, Numayama-Tsuruta K, Maekawa M (2008) Concise review: Pax6 transcription factor contributes to both embryonic and adult neurogenesis as a multifunctional regulator. Stem Cells 26(7):1663–1672. doi:10.1634/stemcells.2007-0884
66. Azimzadeh J, Bornens M (2007) Structure and duplication of the centrosome. J Cell Sci 120(Pt 13):2139–2142. doi:10.1242/jcs.005231
67. Bornens M (2012) The centrosome in cells and organisms. Science 335(6067):422–426. doi:10.1126/science.1209037
68. Meraldi P, Nigg EA (2002) The centrosome cycle. FEBS Lett 521(1–3):9–13
69. Shinohara H, Sakayori N, Takahashi M, Osumi N (2013) Ninein is essential for the maintenance of the cortical progenitor character by anchoring the centrosome to microtubules. Biol Open 2(7):739–749. doi:10.1242/bio.20135231
70. Corbit KC, Shyer AE, Dowdle WE, Gaulden J, Singla V, Chen MH, Chuang PT, Reiter JF (2008) Kif3a constrains beta-catenin-dependent Wnt signalling through dual ciliary and non-ciliary mechanisms. Nat Cell Biol 10(1):70–76. doi:10.1038/ncb1670
71. Gerdes JM, Liu Y, Zaghloul NA, Leitch CC, Lawson SS, Kato M, Beachy PA, Beales PL, DeMartino GN, Fisher S, Badano JL, Katsanis N (2007) Disruption of the basal body compromises proteasomal function and perturbs intracellular Wnt response. Nat Genet 39(11):1350–1360. doi:10.1038/ng.2007.12
72. Muzio L, DiBenedetto B, Stoykova A, Boncinelli E, Gruss P, Mallamaci A (2002) Emx2 and Pax6 control regionalization of the preneuronogenic cortical primordium. Cereb Cortex 12(2):129–139
73. Epstein JA, Glaser T, Cai J, Jepeal L, Walton DS, Maas RL (1994) Two independent and interactive DNA-binding subdomains of the Pax6 paired domain are regulated by alternative splicing. Genes Dev 8(17):2022–2034
74. Muhlfriedel S, Kirsch F, Gruss P, Chowdhury K, Stoykova A (2007) Novel genes differentially expressed in cortical regions during late neurogenesis. Eur J Neurosci 26(1):33–50. doi:10.1111/j.1460-9568.2007.05639.x